MONITORING SNOW COVER OVER EUROPE WITH METEOSAT SEVIRI

Peter Romanov[1,2] , Dan Tarpley[2]

[1] Earth System Science Interdisciplinary Center, University of Maryland
2207 Computer and Space Sciences Building, College Park, Maryland, USA
[2] NOAA/NESDIS, Office of Research and Applications

ABSTRACT

An automated algorithm has been developed to generate maps of snow cover over Europe from Meteosat-8 SEVIRI data. Snow identification technique is based on satellite observations in the visible, near-infrared, shortwave-infrared and infrared. Besides spectral criteria, the algorithm utilizes information on temporal variation of the scene temperature and reflectance in order to improve discrimination between snow and clouds in the satellite imagery. Snow maps are produced on a daily basis since January 2005.

In the paper we give an overview of the developed snow mapping algorithm and analyze the system performance during the second half of the 2004-2005 winter season. To assess the accuracy of snow maps, snow retrievals are compared to reports from ground stations and to NOAA operational interactive snow cover analysis data.

Introduction

Mapping and monitoring snow cover is one of important applications of satellite observations in the visible and infrared. For more than 30 years NOAA has produced charts of snow cover distribution based on a visual analysis of satellite imagery [Ramsey, 2000]. A number of automated techniques to identify and map snow cover have been developed and applied to observations from polar orbiting and geostationary satellites (Hall et al. [2002], Dozier [1989]). In contrast to interactive techniques, automated algorithms better utilize potentials of satellite observations, particularly their high spatial resolution and multispectral observing capability.

Most earlier snow detection and mapping techniques have been developed and tested over the data from polar orbiting satellites. For many years coarse spatial resolution and the lack of observations in the shortwave infrared or in the middle infrared from geostationary satellites have been making attempts to use them for an automated snow monitoring unattractive. Improvement of imaging instruments onboard geostationary satellites in the last decade has brought their spatial resolution and spectral coverage close to the one of polar orbiting satellites and thus has substantially enhanced potentials of geostationary satellites for providing information on the snow cover. At NOAA observations from the Imager instrument onboard Geostationary Operational Environmental Satellites (GOES) have been successfully used within an automated algorithm to routinely map the snow cover distribution over North and South America (Romanov et al, [2000] and [2003]). Automated identification and mapping of snow cover has also become possible from

Meteosat satellite platforms with the launch of Meteosat Second Generation (MSG) carrying the Enhanced Visible and Infrared Imager (SEVIRI).

In this work we present an algorithm to identify snow cover using observations from SEVIRI instrument onboard MSG. The performance of the developed algorithm was examined during the first half of the year 2005. To assess the accuracy of snow maps, snow retrievals were compared to reports from ground stations and to the NOAA operational interactive snow cover analysis data.

MSG snow detection and mapping technique

The developed technique for snow cover identification uses SEVIRI observations in the visible (channel 1, centred at 0.6 μm), near-infrared (channel 2 centred at 0.8μm), shortwave infrared (channel 3, centred at 1.6 μm) and infrared (channel 9, centred at 10.8 μm) spectral bands. Since clouds are generally opaque in the visible, mid-infrared and infrared spectral bands, the retrievals are limited to cloud-clear scenes. A complete data processing scheme to derive maps of snow fraction involves several stages (see Fig.1).

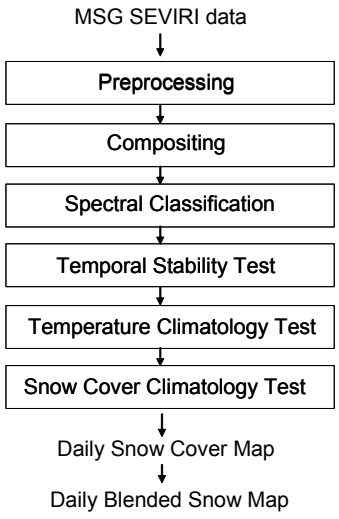

Fig.1 Flow chart of MSG snow mapping algorithm

At the preprocessing stage SEVIRI images acquired every 30 minutes are registered to a latitude-longitude projection with a 0.040 by 0.040 grid size, or approximately 4km spatial resolution. Satellite observations are processed over the area extending from 25^{o} N to 66^{0} N and from 25^{0}W to 55^{0} E. Extending the area further north and east is not feasible because of large satellite view zenith angles. Daytime SEVIRI images acquired during a day are then composited and observations with maximum infrared brightness temperature are retained in every map grid cell. Since the "warmest" observation is most often the least cloud-contaminated, this procedure provides an effective cloud-clearing of the composited image.

Both the daily composited image and all individual 30-minute instantaneous images acquired during a day are further utilized in the snow identification procedure. This procedure uses both spectral signatures and temporal stability criteria to ensure the most accurate image classification and snow mapping. First, the daily composited image is subjected to a threshold-based decision-tree unsupervised spectral-based classification, which separates the image pixels into "snow", "snow free land surface" and "cloud" categories. Besides the brightness temperature in SEVIRI channel 9 (T9), visible and shortwave-infrared reflectance (R1 and R3 respectively) the classification algorithm utilizes a "snow index" (SI, defined as the ratio R1/ R3). The idea of using the ratio of the visible to the middle-infrared or short-wave infrared reflectance to identify snow in satellite images was put forward about two decades ago (see Bunting and d'Entremont [1982]). Due to a low reflectance of the snow cover in the middle infrared and a high reflectance in the visible, the snow index enhances the difference of the spectral response of the snow cover from the response of other surfaces and is thus beneficial for snow detection.

The sequence of spectral tests included in the snow identification algorithm is shown in Figure 2. Fixed threshold values were used for SI (SI_T=1.2) and T9 ($T9_T$=290^{0} K), whereas for the visible and shortwave infrared reflectance, the threshold values ($R1_T$ and $R3_T$) were assumed to be location dependent and were defined for every grid cell of the map. To establish $R1_T$ and $R3_T$ and the model approximating the land surface reflectance anisotropy in the visible and in the shortwave infrared we have used statistics of MSG cloud-clear observations accumulated during snow-free periods of the first half of the year 2005. Values of $R1_T$ and $R3_T$ for a grid cell were set equal to

values exceeding the average visible and shortwave infrared reflectance for this grid cell by twice the standard deviation. The land surface reflectance anisotropy was characterised using a semi-empirical kernel-driven model of Roujean et al. (1992). The model is governed by two coefficients, which are the loadings on the kernels representing correspondingly volumetric scattering and surface geometrical effects, and a constant.

After snow-covered pixels are separated, the image classification procedure continues with discriminating non-snow pixels into “clouds” and “snow free land surface”. Observations having a low (below 265 K) brightness temperature or a moderate brightness temperature (within 265K to 285K) along with a high visible reflectance, high shortwave infrared reflectance and low normalized difference vegetation index (NDVI=(R2-R1)/(R2+R1)) are labelled as “cloudy”. All remaining image pixels are assigned a “snow free land surface” flag.

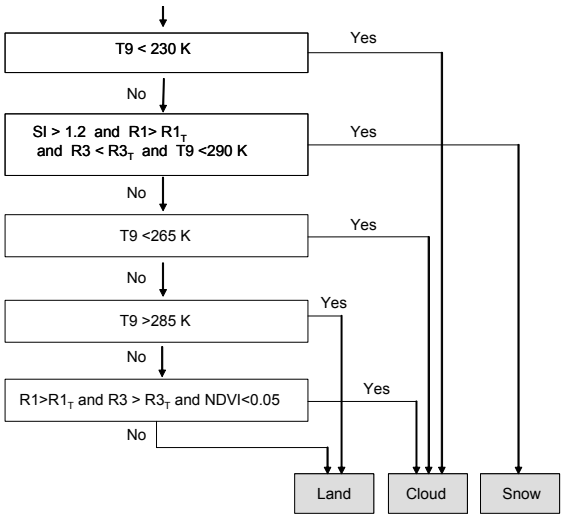

Fig.2 MSG image classification algorithm

Experience with numerous MSG SEVIRI scenes has shown that some clouds exhibit spectral features similar to snow and thus cannot be distinguished from snow cover only from instantaneous spectral measurements. To resolve this ambiguity, we complemented the image classification algorithm with a temporal stability test (see Fig.1). In this test an intra-day temporal variability of the scene temperature and reflectance is employed as a predictor to distinguish between cloudy and cloud clear pixels. The test is applied only to those image pixels, which were classified as “snow covered” according to their spectral response. For every “snow covered” pixel, the “warmest” observation retained in the daily composite is compared to all observations over this location acquired during the day. The pixel is confirmed as “snow”, if three or more instantaneous observations are found, which are spectrally similar to the “warmest” one. Observations are considered similar if corresponding values of R1 and T9 are within 5% and 8 K, respectively. These threshold values were determined empirically through a visual examination of satellite imagery and quantitative analysis of daily time series of satellite observations over selected targets representing different surface types. It should be noted that the values of thresholds given above are very close to corresponding threshold values proposed by Key and Barry [1989] to detect clouds over snow covered land surface in the polar area from a series of daily NOAA AVHRR images.

In order to further improve the removal of falsely identified snow cover we applied two additional tests based on the land surface temperature climatology and the snow cover climatology. Snow identified in the satellite imagery is rejected if the scene infrared brightness temperature is more than 20^0K below its climatic value for a given location and the time of the year or if for the given time of the year snow cover was never observed before within a 2^0 by 2^0 area centred on the pixel location. The land surface temperature monthly climatology was adopted from the International Satellite Cloud Climatology Project (ISCCP), whereas the snow cover statistics was calculated from NOAA weekly snow cover charts for the period from 1972 to 2004.

Portions of a daily automated snow map are typically contaminated with clouds. In order to facilitate qualitative analysis of the snow cover distribution over the whole continent we have also generated blended daily snow cover maps. These maps were obtained by filling in cloudy portions of a current day snow map with the most recent cloud-clear classifications.

Results

Using the algorithm described above, daily maps of snow cover over Europe have been produced since January 2005. The area covered by snow maps was confined to within 25^0N to 66^0N and 25^0W to 55^0E. Figure 3 presents an example of an MSG-based snow cover map derived on February 10, 2005. Following a series of snow storms that affected Europe in the beginning of February, snow cover extended to most of Central and Eastern Europe, Eastern Turkey and Northern Iran. Satellite-based snow map also reveals snow cover over Atlas Mountains in Northern

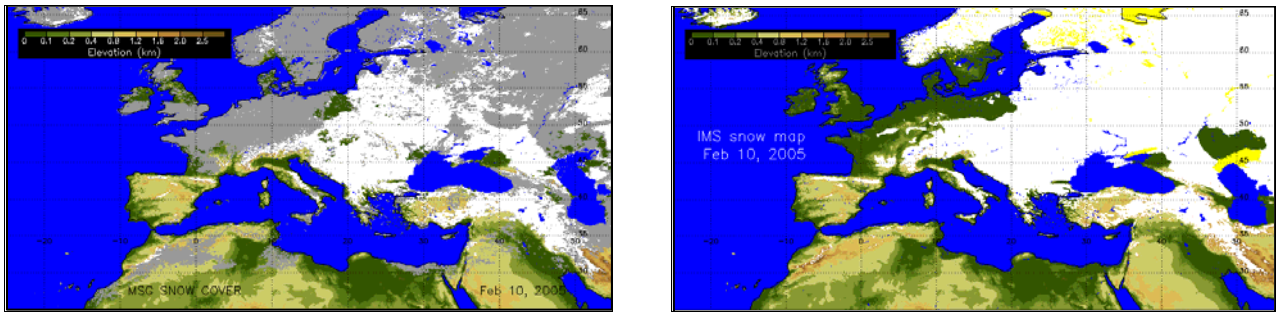

Fig.3 Snow cover maps for February 10, 2005. Left: automated MSG-based snow map, Right: NOAA Interactive snow cover map over Europe. White is snow, grey is clouds. Yellow colour in the IMS map represents ice. Surface elevation is shown in the background with shades of green and brown.

Africa. In cloud clear portions of the image the satellite-derived snow cover distribution agrees well to the snow cover map generated interactively within NOAA Interactive Snow and Ice Mapping System (IMS) (see Fig.3). There are minor differences in two products along the western coast of Black Sea and in Central Europe where the MSG-based snow map shows patches of snow-free land while the IMS map presents continuous snow cover. The interactive snow cover map also shows somewhat more snow over mountainous areas of Apennine and Iberian Peninsular.

A closer view on a mountainous area in Eastern Turkey (Fig.4) reveals small-scale differences in the automated and interactive snow map. The automated product captures most of peculiarities of the snow distribution correctly however the derived snow cover distribution appears to have lower spatial resolution than in the interactive product. A decrease in the effective spatial resolution is most probably caused by high, over 60^0, zenith angle of satellite observations over this area. At this angle the size of the instrument field of view on the ground surface exceeds 10 km whereas

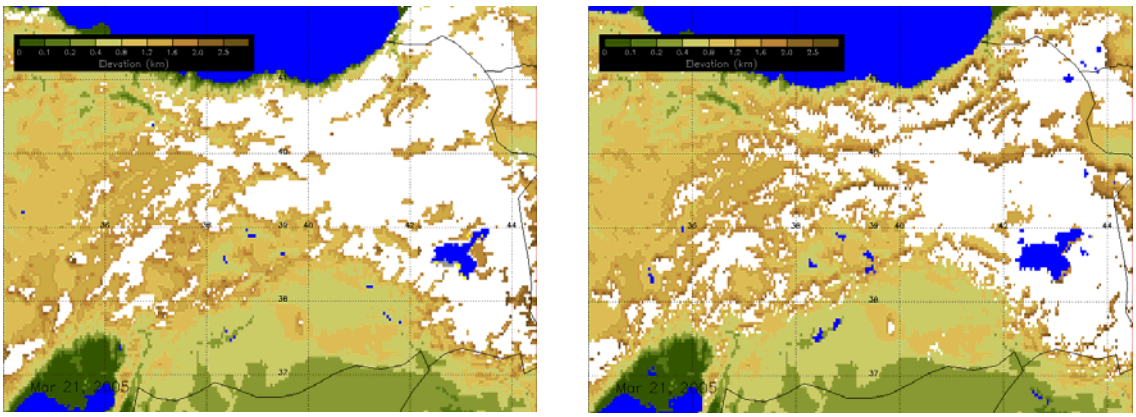

Fig.4 Snow cover maps over Eastern Turkey for March 21, 2005. Left: automated MSG-based snow map, Right: NOAA Interactive snow cover map over Europe. Snow cover is shown in white.

the resolution of the interactive map is 4 km.

Figure 5 compares daily estimates of snow covered area over Eastern Turkey derived from automated and interactive snow cover maps. MSG-based estimates of the snow covered area were derived from daily blended snow cover maps. Despite some differences in the spatial distribution of snow cover in two products (interactive and automated) mentioned above they agree well on the extent of snow. Except of few days in the beginning of February, corresponding to a sharp drop in the estimated snow-covered area in the interactive product, the difference between snow extent estimates did not exceed 10%. There are obvious steps in the graph for the snow extent derived from the interactive snow map. This indicates that although the IMS product is delivered daily, analysts do not revisit the area and hence do not introduce updates to the snow cover distribution on a daily basis.

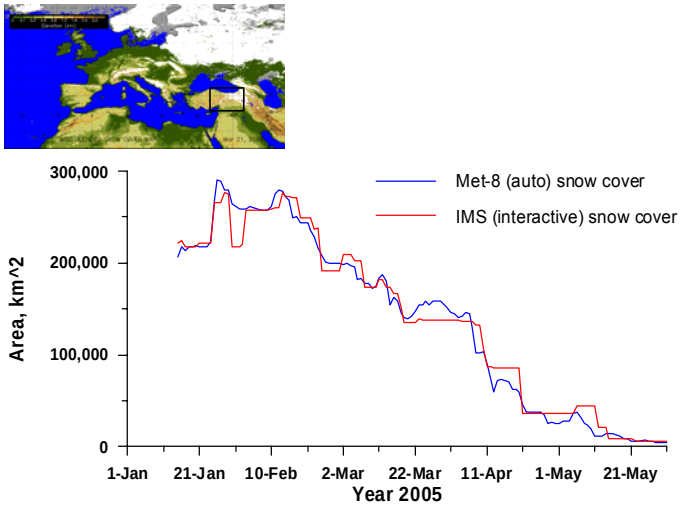

Fig.5 Snow extent over Eastern Turkey estimated from automated (MSG-based) and interactive (IMS) snow maps.

Another way for assessing the performance of the automated snow mapping algorithm and the accuracy of MSG snow maps consists in their comparison with synchronous ground-based observations of snow cover. There are several hundred manually controlled meteorological stations reporting snow depth in winter within the domain of MSG observations. To qualitatively evaluate the accuracy of derived snow cover distribution we have generated daily snow maps with overlaid surface observation data. An example of such map presented in Fig. 4a demonstrates a reasonable agreement of the two datasets. Overall, snow cover observed on the ground is confirmed by MSG in 95% to 100% of cases during most of the snow season. The accuracy of snow cover identification noticeably decreases towards the end of winter season. In late spring (late April-May) snow cover remains only in forested areas of North-East of Russia and in the North of Scandinavia. Detection of snow in satellite images in these areas is hampered by large satellite view zenith angles exceeding 70^0 and by dense forests which tends to mask snow. The accuracy of snow cover identification in the interactive product averaged over the whole winter seasons is very close to the one of the

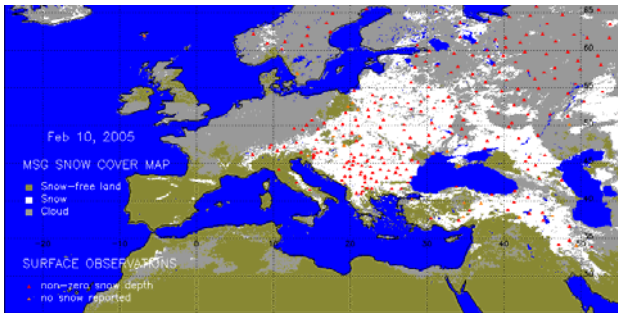

(a)

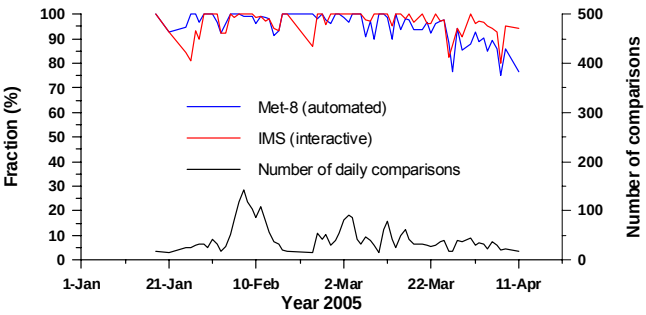

(b)

Fig. 6 (a): MSG-based snow cover map with overlaid surface observations. Red triangles represent stations reported non-zero snow depth, yellow triangles are stations reported no snow on the ground. (b): Fraction of correct snow identifications in the automated and in the interactive snow cover product.

automated product (95% and 94%, respectively), however the interactive product exhibits better correspondence to surface observations in the end of the winter season. This is explained by the fact that when mapping snow cover over high latitudes IMS analysts rely on images both from geostationary and polar orbiting satellites. Closer to nadir views from polar orbiting satellites facilitate identification of patchy and shallow snow cover in forests.

The results presented above characterise the performance of the snow detection and mapping algorithm during late winter and spring. These seasons are most favourable for snow cover monitoring with satellite observations in the visible and infrared due to high solar elevation and extended daylight conditions. Mapping snow in the fall and in winter season may present more problems. Lesser number of observations made in daylight conditions and more extensive cloud cover may affect the ability to accurately and timely represent changes in the snow cover distribution.

Summary

An automated algorithm has been developed to identify snow in MSG imagery. Daily snow maps over Europe have been routinely generated since January 2005. Satellite derived maps of snow cover distribution have shown a good agreement to snow maps derived interactively at NOAA NESDIS. Comparison of automated snow maps with surface observation data has shown that snow cover observed on the ground is correctly identified from satellite in about 95% of all retrievals.

The described technique is currently subjected to further testing to evaluate its performance in the fall season.

References

Bunting, J.T. and R.P. d'Entremont (1982) Improved cloud detection utilizing defense meteorological satellite program near infrared measurements, Air Force Geophysics Laboratory, Hanscom AFB, MA, AFGL-TR-82-0027, Environmental Research Papers, No. 765, 91 p.

Dozier, J., Spectral signature of alpine snow cover from the Landsat Thematic Mapper (1989) Remote Sensing of Environment, 28 (1), 9-22.

Hall, D.K., G. Riggs, V. Salomonson, N.E.DiGirolamo and K.J.Bayr (2002) MODIS snow cover products, Remote Sens. Environ., 83, 181-194.

Ramsay, B., (1998) The interactive multisensor snow and ice mapping system Hydrolog. Process., 12, 1537-1546.

Romanov P., G. Gutman and I. Csiszar, Automated monitoring of snow cover over North America with multispectral satellite data (2000) J. Appl. Meteorol. 39, 1866-1880.

Roujean, J.-L., M. Leroy, and P.Y. Deschamps (1992) A bidirectional reflectance model of the Earth's surface for the correction of remote sensing data. J. Geoph. Res., 97D, 20455-20468.